Supplementary materials

Evaluating the antimicrobial activity and cytotoxicity of polydopamine capped silver and silver/polydopamine core-shell nanocomposites

Ndivhuwo P. Shumbula[a], Siyabonga S. Nkabinde[a], Zakhele B. Ndala[a], Siyasanga Mpelane[b], Morgan P. Shumbula[c], Phumlani S. Mdluli[d], Zikhona Njengele-Tetyana[e], Phumlani Tetyana[d], Thulani Hlatshwayo[f], Mbuso Mlambo[*g], Nosipho Moloto[*a]

[a] Molecular Sciences Institute, School of Chemistry, University of the Witwatersrand, Private Bag 3, Wits, 2050, South Africa

[b]Analytical Facility, University of Johannesburg, P.O. Box: 524, Auckland Park 2006, South Africa

[c]Department of Chemistry, University of Limpopo, Private Bag x1106, Sovenga 0727, South Africa

[d] DST/Mintek NIC, Advanced Materials Division, Mintek, 200 Malibongwe Drive, Randburg, South Africa,

[e]Center for Metal-Based Drug Discovery, Advanced Materials Division, Mintek, 200 Malibongwe Drive, Randburg, South Africa

[f]Physics Department, University of Pretoria, Pretoria 0002, South Africa

[g] Institute for Nanotechnology and Water Sustainability, College of Science, Engineering and Technology, University of South Africa, Florida Science Campus, 1710, South Africa

[*]Corresponding authors: Mbuso Mlambo and Nosipho Moloto

Tel: +2711 717 6774

E-mail address: mlambm@unisa.ac.za; nosipho.moloto@wits.ac.za

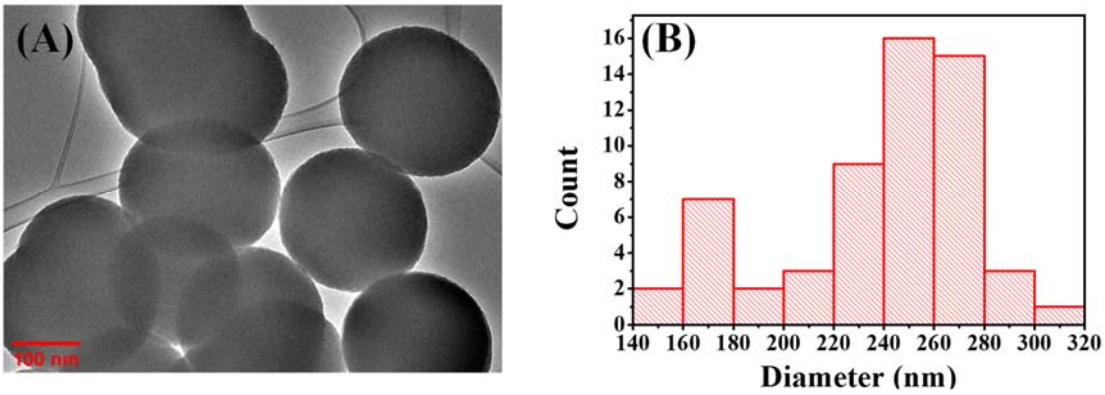

Figure S1: TEM micrograph (A) and particle size distribution (B) of PDA spheres

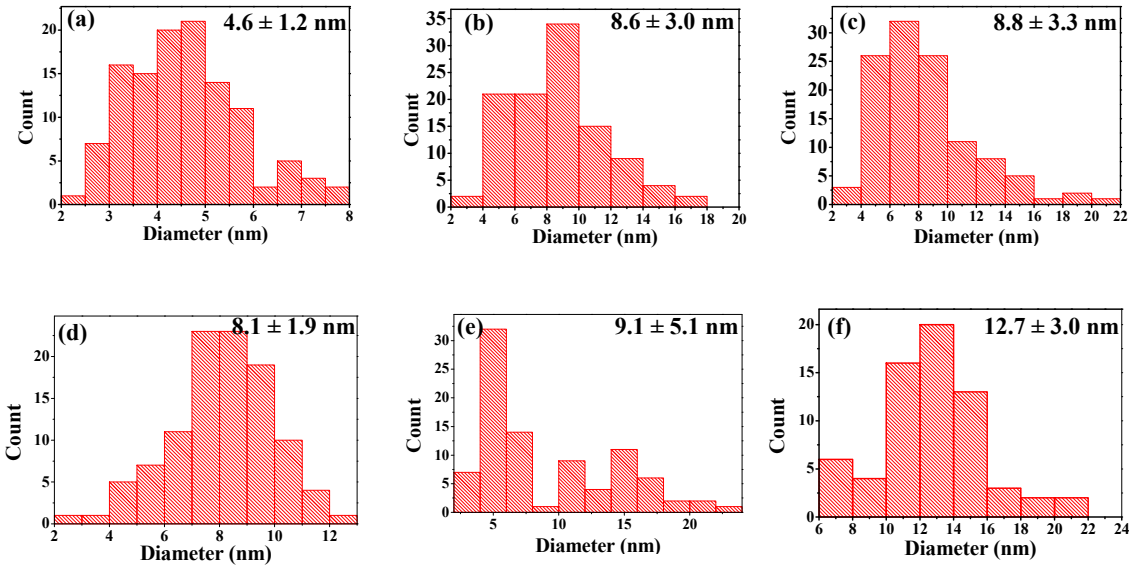

Figure S2: Particle size distributions of (a-c) Ag-PDA and (d-f) Ag@PDA nanocomposites at different $AgNO_3$ concentrations. [**(a, d)** 1 mM, **(b, e)** 5 mM and **(c, f)** 10 mM].

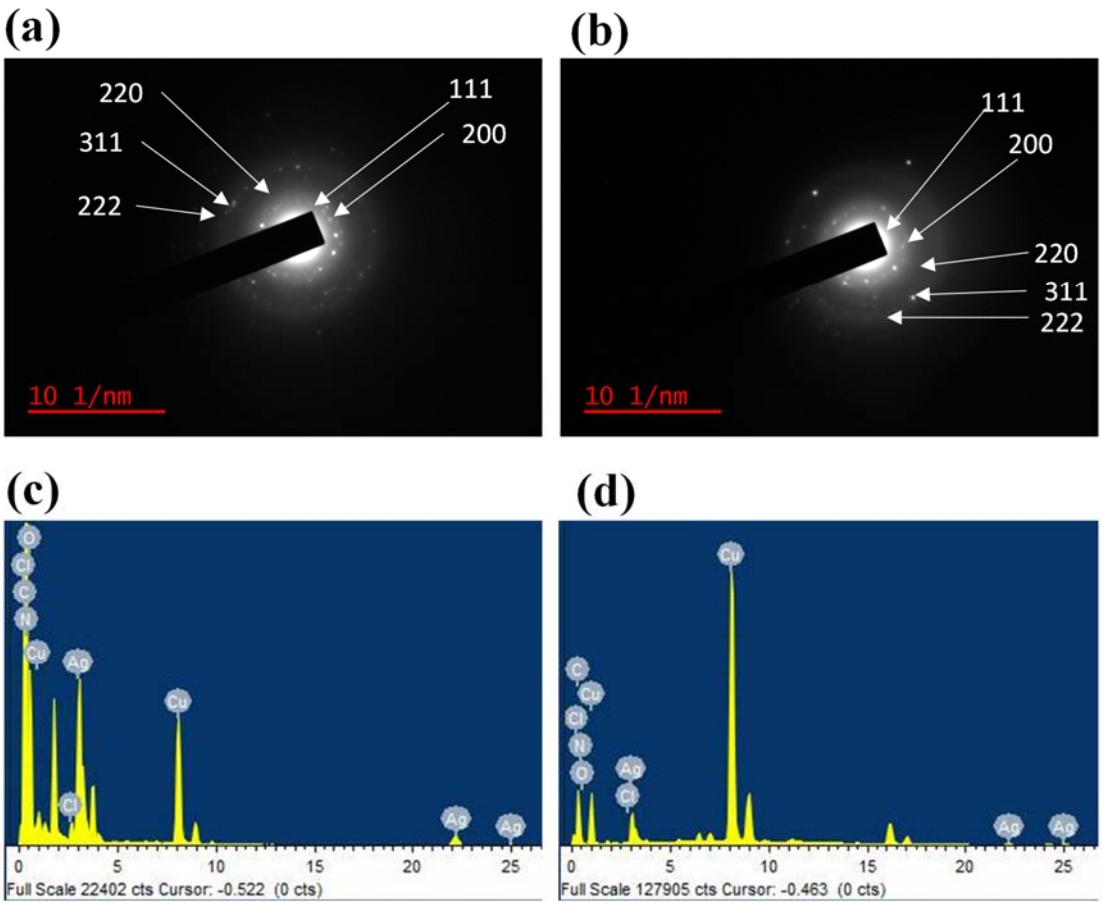

Figure S3: SAED and EDS of (a, c) Ag@PDA and (b, d) Ag@PDA nanocomposites [At $AgNO_3$ concentrations of 1 mM].

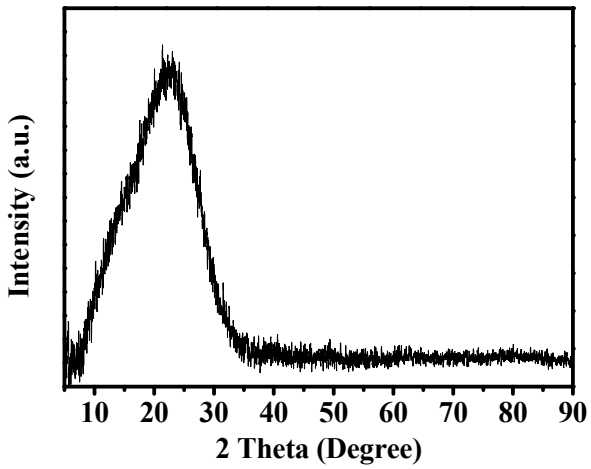

Figure S4: PXRD pattern of PDA spheres

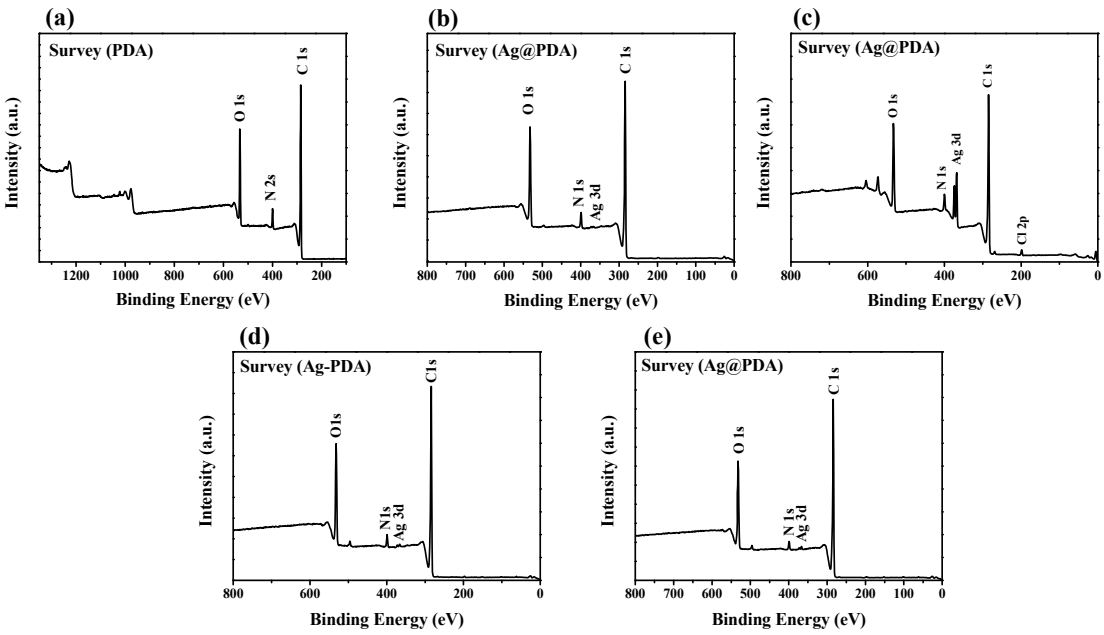

Figure S5: The XPS survey spectra of (a) PDA, (b) Ag@PDA [1 mM], (c) Ag@PDA [10 mM], (d) Ag-PDA [1 mM] and (e) Ag-PDA [10 mM].

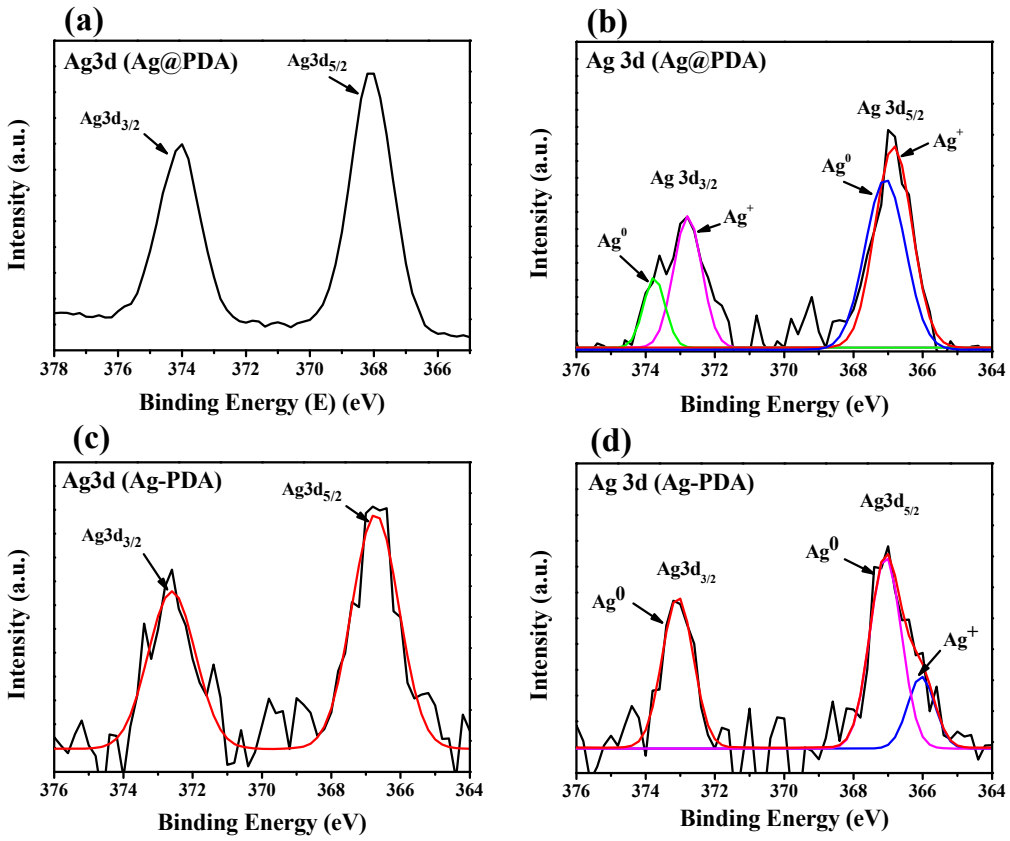

Figure S6: Ag3d high resolution XPS spectra of (a) Ag@PDA [1 mM], (b) Ag@PDA [10 mM], (c) Ag-PDA [1 mM] and (d) Ag-PDA [10 mM].

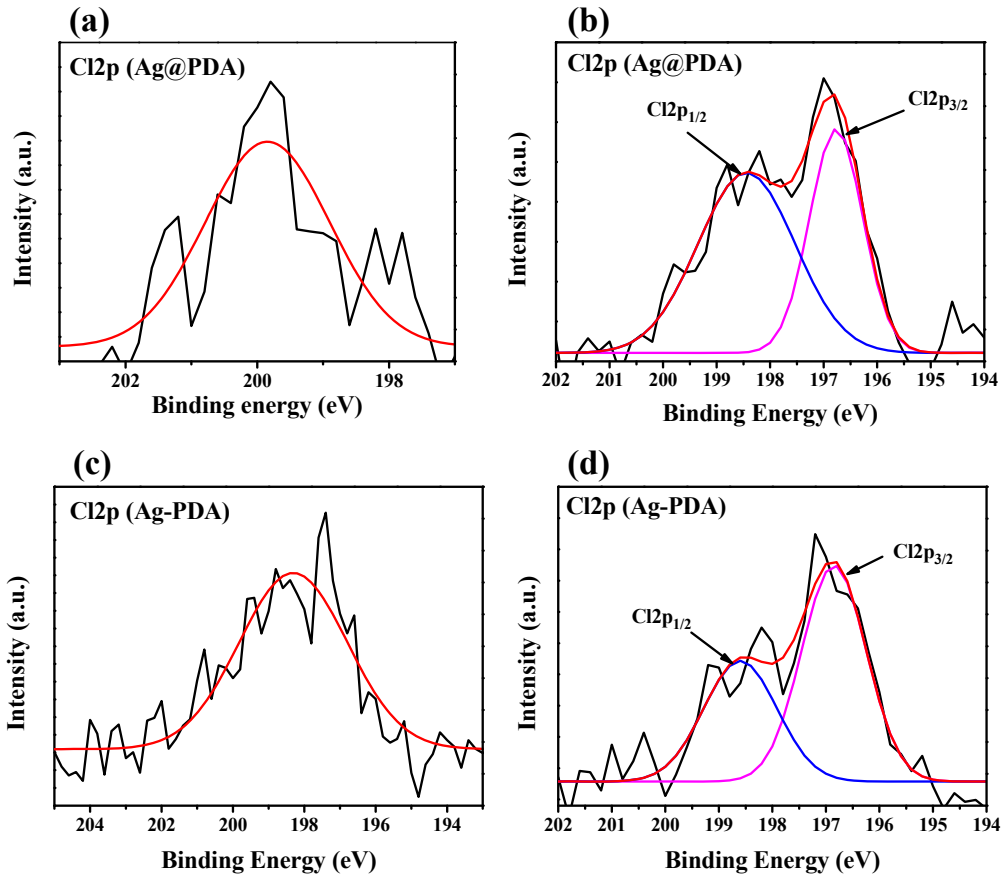

Figure S7: Cl 2p high resolution XPS spectra of (a) Ag@PDA [1 mM], (b) Ag@PDA [10 mM], (c) Ag-PDA [1 mM] and (d) Ag-PDA [10 mM].

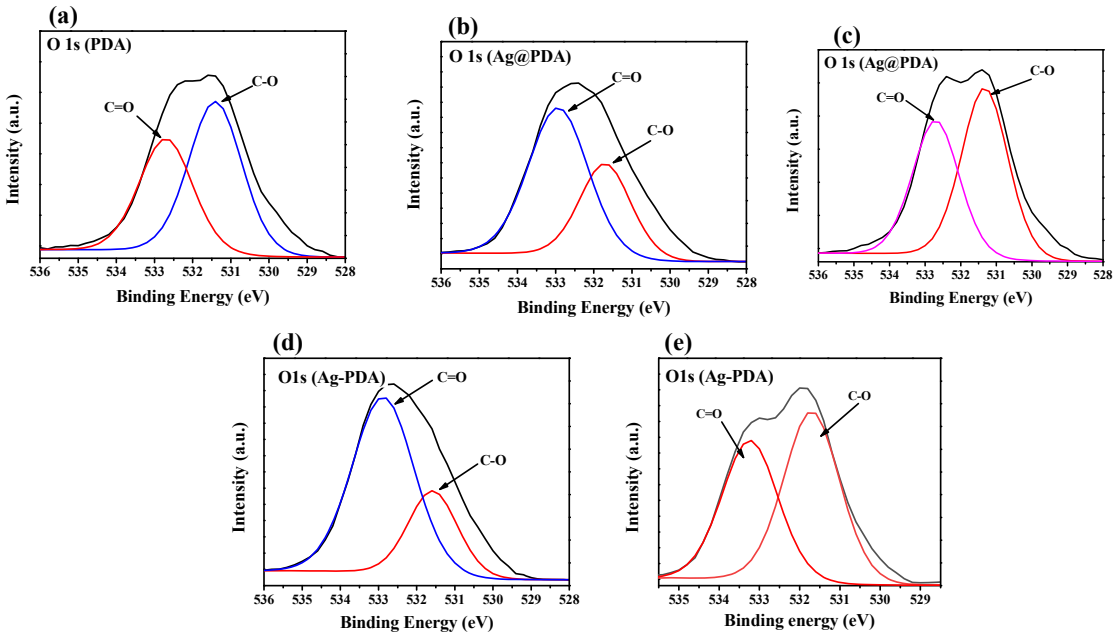

Figure S8: O 1s high resolution XPS spectra of (a) PDA, (b) Ag@PDA [1 mM], (c) Ag@PDA [10 mM], (d) Ag-PDA [1 mM] and (e) Ag-PDA [10 mM].

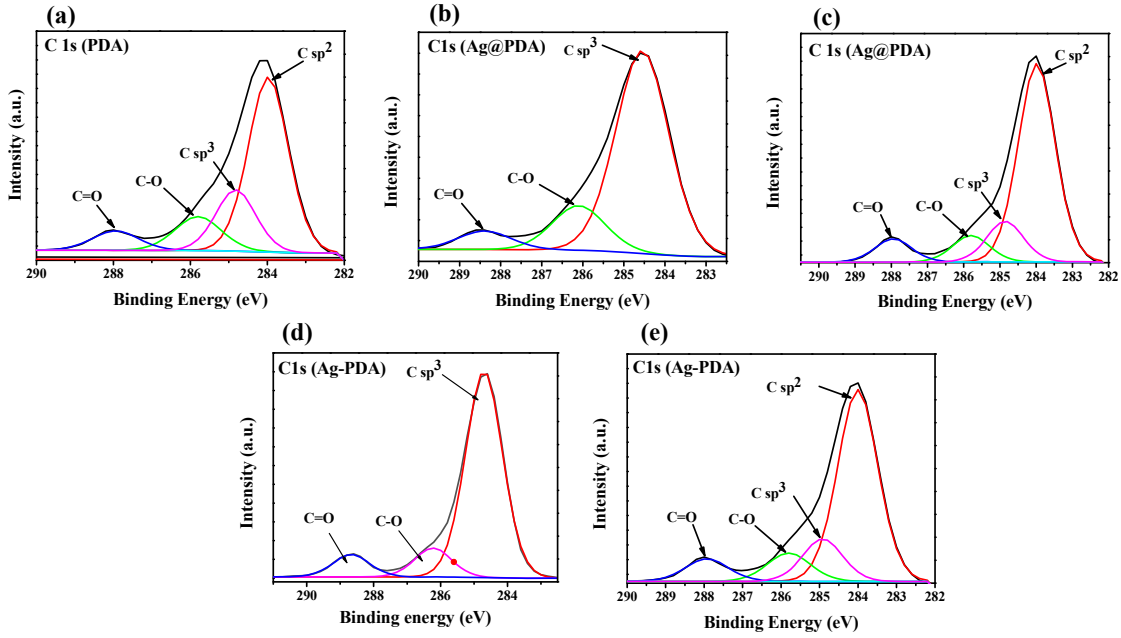

Figure S9: C 1s high resolution XPS spectra of (a) PDA, (b) Ag@PDA [1 mM], (b) Ag@PDA [10 mM], (d) Ag-PDA [1 mM] and (e) Ag-PDA [10 mM].

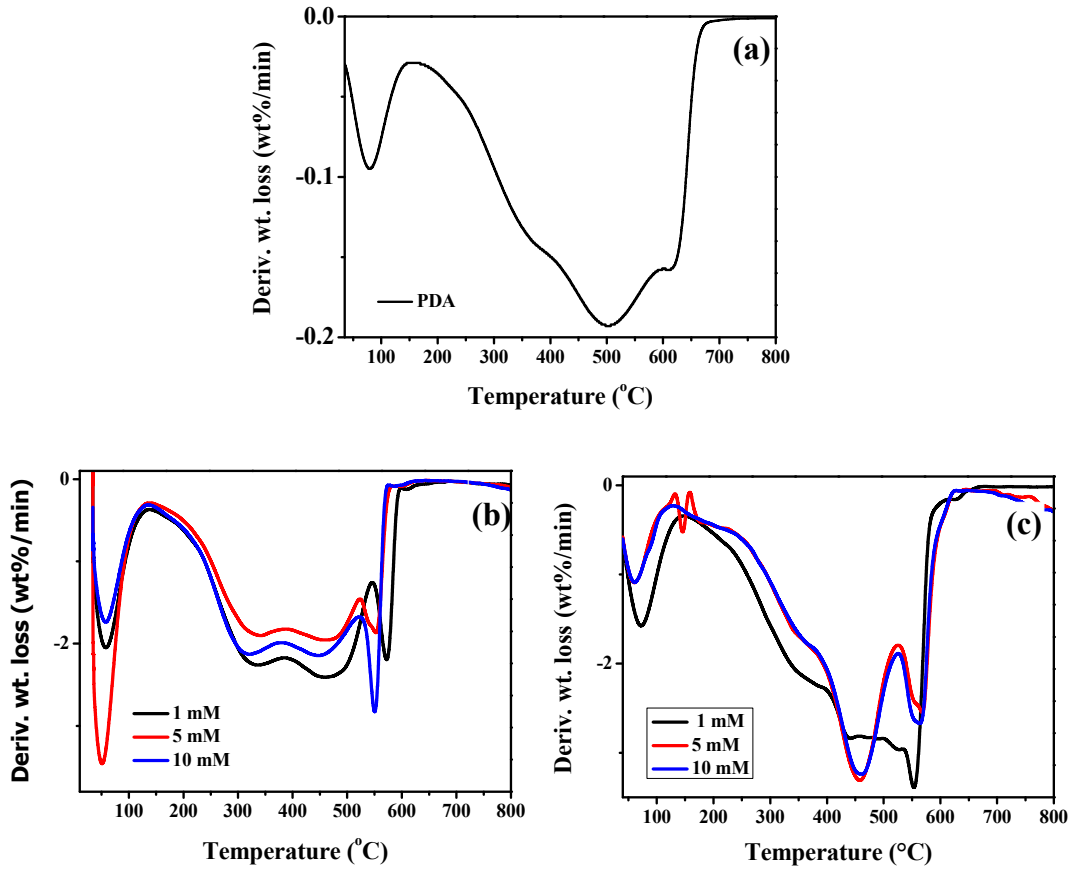

Figure S10: DTGA of (A) PDA. (B) Ag-PDA and (C) Ag@PDA nanocomposites at different $AgNO_3$ concentrations.

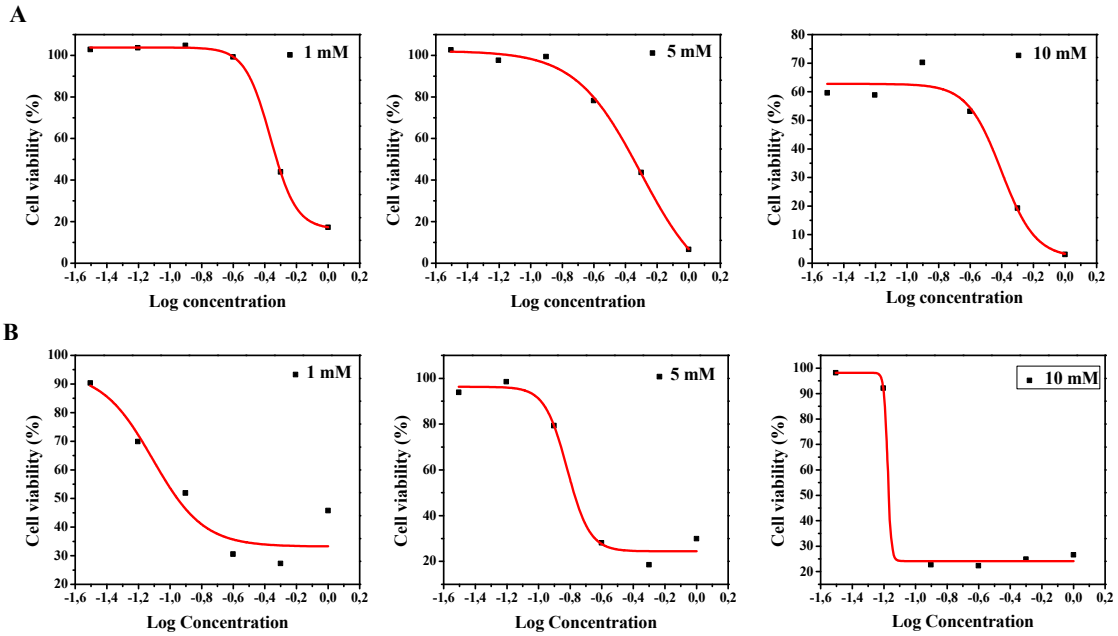

Figure S11: Sigmoidal curves used to determine the CC_{50} values of (A) Ag-PDA and (B) Ag@PDA at different concentration of $AgNO_3$.

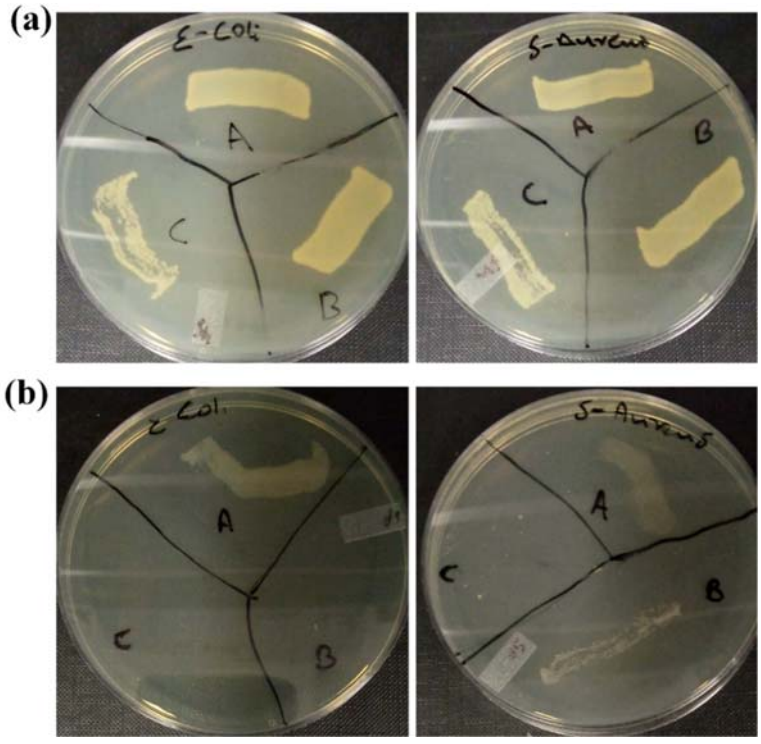

Figure S12: The MBC of (a) Ag-PDA and (b) Ag@PDA nanocomposites at different $AgNO_3$ concentrations [**(A)** 1 mM, **(B)** 5 mM and **(C)** 10 mM]

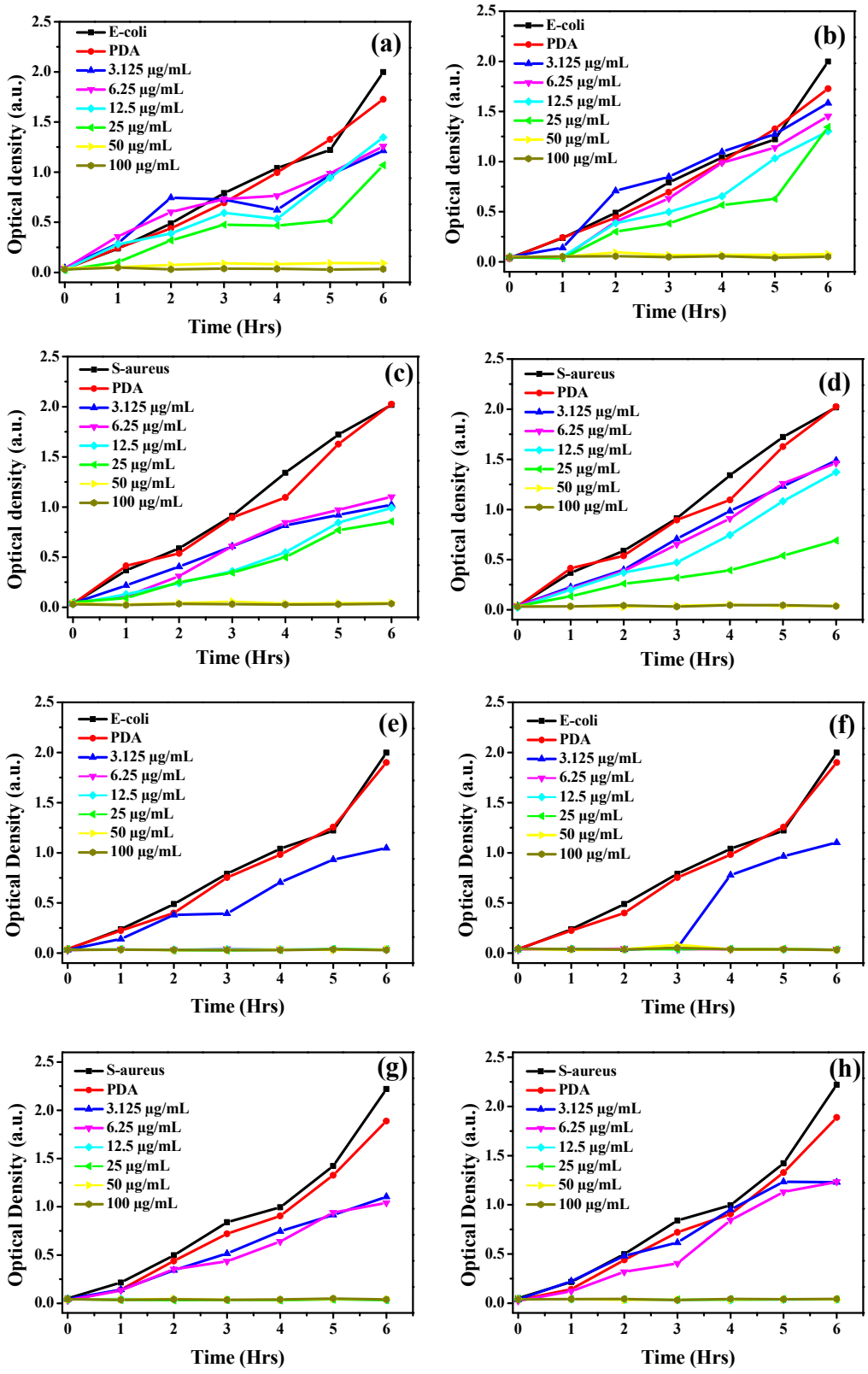

Figure S13: The bacterial growth curves of (A-D) Ag-PDA and (E-F) Ag@PDA against E-coli and S-aureus.